Compact Planar Electromagnetic Bandgap Structure for Signal and Power Integrity Improvement in High-Speed Circuits

Manisha R. Bansode[1, *] **and Surendra S. Rathod**[2]

Abstract—This paper introduces and validates a compact two-dimensional Electromagnetic Bandgap (EBG) structure for the improvement of signal integrity (SI) and power integrity (PI) by suppressing Simultaneous Switching Noise (SSN). SSN bandwidth can be increased by using the proposed T bridge compact planar structure. The proposed structure is simulated using Ansys HFSS Software. Simulated and measured results by Vector Network Analyzer provide 3.13 GHz to 11.40 GHz frequency bandgap with good mitigation of SSN at -30 dB noise suppression reference. It will almost cover S, C, and X bands from electromagnetic frequency spectrum. This will be useful for satellite and terrestrial communication and radar communication applications. The proposed structure analyzes signal integrity issues using eye diagram in MATLAB and power integrity in HFSS with input impedance respectively. The main purpose of this work is to provide a compact structure to improve signal and power integrity by the suppression of power/ground noise. Comparative study is also performed with the proposed structure and reference board with similar dimensions.

1. INTRODUCTION

Nowadays, the high-speed design in GHz band has a main focus on signal integrity and power integrity of a system. Work gets more difficult for electronics business as a result of decreased voltage levels, cost efficiency, miniature size, and higher data rate of a system. System operates as per decided design guidelines for lower frequency, but system issues including reflection, ringing and crosstalk, and other electromagnetic interferences will become worse as frequency rises. Due to clock frequency and data rate rising continuously, simultaneous switching noise (SSN), a major problem, is growing for higher frequency applications. Due to cavity mode resonance on the parallel plate waveguide power planes of the high-speed printed circuit boards and the Power Distribution Network (PDN), simultaneous switching noise (SSN) is an undesired voltage fluctuation emerging [1–3]. There are signal integrity and power integrity problems that arise due to resonance modes in power and ground planes. Other significant problems in high-speed circuits and PCBs include power integrity, electromagnetic interference, and signal integrity. Researchers found effects of these issues in both time and voltage domain. Therefore, It is necessary to maintain signal and power integrity in electronics systems. By changing the timing of the system, we can reduce the impact of noise [4–6].

For the suppression of electromagnetic interference, many solutions are found like the use of decoupling capacitors, splitting planes, differential interconnection, and shorting vias. Typically, decoupling capacitors are positioned on top of the PCB. To separate high frequency oscillations from the power plane, capacitors are positioned close to the noise source. At specified frequencies, it establishes a low impedance path between the planes.

High Impedance Surfaces (HIS), such as Electromagnetic Band Gap (EBG) and Photonic Band Gap (PBG) structures, minimize simultaneous switching noise. Due to its unique surface wave suppression capabilities, EBG has been found to be beneficial in numerous applications, including antennas and microwaves. EBG structures have periodic patches that are mushroom-shaped, and vias are utilized to connect the patches to the ground [7]. Wide bandgap for high-speed circuits has been proposed using hybrid EBG structures by combining two or more structures [8–11]. Electromagnetic bandgap structures are more popular mainly for compact size helpful for system packages and other bandgap bandwidth improvement by mitigating the SSN effect at higher frequency. The power/bus noise from printed circuit boards is overcome using several forms of planar EBG designs [12–20]. Using a series of patches attached to various types of bridges or meander lines reduces noise in high-speed circuits [21–25]. With the above literature survey, we can observe that more focus is on the widening of bandwidth and suppression of SSN.

In this paper, a periodic two-dimensional EBG structure is designed for the improvement of signal integrity and power integrity in high-speed design applications to achieve wide bandgap. Power plane and ground plane are continuous solid planes, and the structure is formed of periodic patterns. The bandgap, signal quality, and power integrity are all improved by using a T-bridge arrangement between two single cells. A finite element software is used to carry out this design and analysis (Ansoft HFSS). The main purpose of this work is to examine the noise-reduction capabilities of EBG structure with intrinsic stopband with high attenuation, so that it can be used successfully in high-speed circuits, high-speed PCBs, satellite communication, and radar communication to increase bandgap with improved power integrity. Planar EBG structure is cost effective because it can be fabricated by standard PCB fabrication technique.

The organisation of this paper is as follows. The design of the proposed compact planar EBG structure is covered in Section 2. Power ground noise mitigation performance is explained in Section 3. Power integrity of the proposed structure is shown in Section 4. Signal integrity of the proposed structure is shown in Section 5. Hardware implementation and Validation of the proposed structure are addressed in Section 6. The paper is concluded in Section 7.

2. DESIGN OF COMPACT PROPOSED PLANAR EBG STRUCTURE

A wider bandgap in the transmission characteristics is produced by an electromagnetic bandgap (EBG) design that interrupts the noise transmission channel at higher frequencies. The two-layer power distribution system in the proposed compact two-dimensional EBG structure has two layers, one of which has a periodic pattern. Eight patches are symmetrically arranged on it. The EBG structure on a flat sheet of metal acts as a high impedance surface with an array of patches bridges connecting them. We assume that EBG structure operates like parallel resonant LC circuits. Helmholtz equations are used to calculate resonance frequencies [16, 26, 27],

$$f_{TM\,pq} = \frac{c}{2\pi\sqrt{\mu r \epsilon r}}\sqrt{\frac{(p\pi)^2}{M} + \frac{(q\pi)^2}{N}} \tag{1}$$

where 'M' is the dimensions, i.e., length of the parallel plate structure; 'N' is the dimensions, i.e., width of the parallel plate structure; and 'c', ϵr, and μr are the velocity of light, velocities of permittivity and permeability. Characteristics impedance can be calculated by [29].

$$Z_0 = \frac{\eta h}{a}\sqrt{\frac{L}{C}} \tag{2}$$

where 'a' is the patch width; 'L' stands for the inductance per volume for the square patch and remaining reference plane component, while 'h' stands for the proposed design dielectric thickness. For the branch and remaining reference plane parts, 'C' represents a capacitance per volume, while η represents the intrinsic impedance of FR4.

For a 2D T-bridge planar structure, stopband frequencies are obtained from [16, 26, 27], which determines the proposed length of patch and width in terms of dimensions,

$$f_{low} = \frac{1}{2\sqrt{\mu r \epsilon r}}\sqrt{\frac{p}{l}} \tag{3}$$

The bridge length is indicated by the letter 'l' in this case. Equation (3) is used to calculate the patch dimensions for the $(N - 1, 0)$ mode of the initial low frequency of the stopband, where N is the number of unit cells. The total number of patches is for a one dimensional view.

$$f_{low} = \frac{1}{2\sqrt{\mu r \epsilon r}}\sqrt{\frac{q}{a}} \tag{4}$$

For the mode value (zero, one) of starting lower frequency of bandgap, patch dimensions calculations are made in accordance with Equation (4). We utilised a square shape, and the higher frequency is determined using Equations (3) and (4).

The designed unit cell, which is square in shape with a and b being 12 mm, is shown in Figure 1. Stopband calculation is done for starting frequency, i.e., lower frequency and ending frequency (higher frequency) from [23] for planar structure. Single patch is connected with adjacent patch by the bridges designed by width and length variations effects and also obtaining wider stopband. Bridge dimensions are determined by the effects of width and length adjustments as well as by monitoring bandwidth improvement. As illustrated in Figure 2, the bridge has the following dimensions: length $g = 2.5$ mm, width $w = 0.2$ mm, T shape length $l = 2.5$ mm, and T shape width $k = 0.4$ mm.
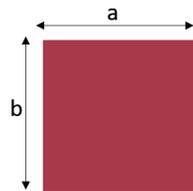

Figure 1. Top view of unit cell proposed planar EBG structure.

The structure shown in Figure 2 has a solid layer for one voltage level and patterned plane for another voltage level. A side view of 2×8 structure is shown in Figure 2(b), and it has an EBG-like periodic top layer and a bottom layer with a continuous ground plane. In addition, a dielectric layer exists between the ground plane and the patterned power plane. There are eight square patches that are connected to one another via bridges. Additional inductive effect is provided by the bridges, and capacitive effect is provided by the patches in the structure, and widened stopband in scattering parameters is observed.
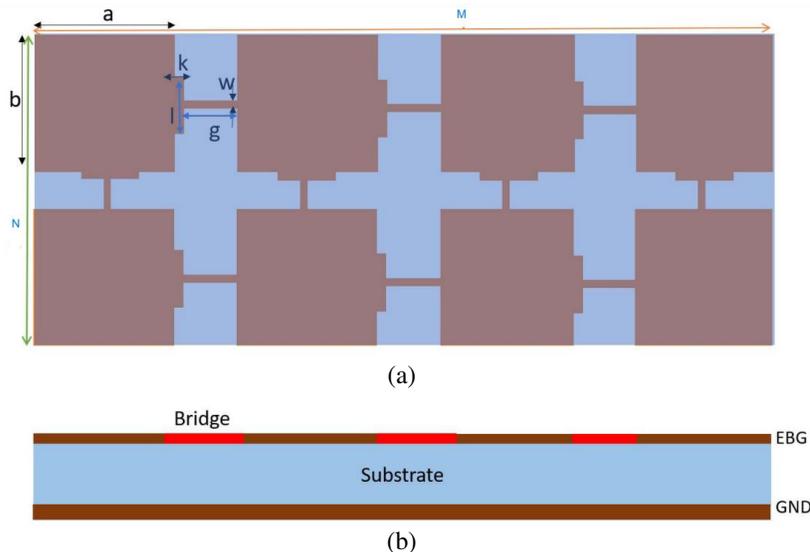

(a)

(b)

Figure 2. T bridge planar EBG structure, (a) geometrical top view, (b) cross sectional view.

The proposed miniature structure provides wide stopband and shows improved signal and power integrity of a system. It is designed of 2×8 unit of dimensions 26.9 mm $\times$ 56.7 mm $\times$ 0.8 mm. As a dielectric material, FR-4 epoxy is utilised, which has a loss tangent (δ) of 0.02 and relative permittivity (ϵr) of 4.4. Checking insertion loss is made easier by specially designed ports. As a noise excitation source, input port "1" is located at (5 mm, 5 mm), and the noise-sensitive component, output port "2" is located at (22 mm, 52 mm). Table 1 includes labels for each dimension of the suggested structure [16]. For the purpose of mitigating simultaneous switching noise, a standard threshold is established. ANSYS High Frequency Structure Simulator is used to simulate the scattering parameter (HFSS) [28].

Table 1. Proposed structure dimentions.

Labels	Initials	Values with units
Length of proposed patch	a	12 mm
Width of proposed patch	b	12 mm
Length of designed substrate	m	55.6 mm
Height of designed substrate	h	0.8 mm
Length of designed bridge	g	2.5 mm
Width of designed bridge	w	0.2 mm
T shape bridge width	k	0.4 mm
Substrate Permitivity	'ϵr'	4.4

One important step is the extraction of equivalent circuit model for planar EBG design [30, 31]. Equivalent circuit is used for the design of one-dimensional structure in Figure 3 as given in [6]. A high impedance parallel plate waveguide is shown by the bridge used to join the patch to the substrate, while a low impedance parallel plate waveguide is shown by the substrate and metal patch. Power plane and EBG patch show the effect of patch capacitance and patch inductance. The designed bridge gives bridge inductance effect between two patches and also gap capacitance effect due to fringing electric field of gap between adjacent patches. The combined effect works like an electric filter for a resonant frequency. Equivalent capacitance (Cp) and equivalent inductance (Lp) represent propagation characteristics between metal patch and the respected ground plane. Equivalent bridge capacitance (Cb) and inductance (Lb) represent bridge connection between two adjacent patches. Parasitic inductance (Lparasitic) and capacitance (Cc) are parameters of chip capacitance and inductance as in [6].

Reference board is without EBG structure, designed as 26.9 mm $\times$ 56.7 mm $\times$ 0.8 mm, same proposed structure dimensions. One output receiver port "2" is located at (22 mm, 52 mm), and one input port "1" is located at (5 mm, 5 mm). We have tested and compared reference and proposed boards with simulation and hardware experiments.

3. SSN MITIGATION PERFORMANCE

Low frequency limit, suppression depth, and suppression bandwidth are required for SSN mitigation. EBG plane gives very good performance on mitigating simultaneous switching noise at higher frequency. Ansoft HFSS is used for scattering parameters calculations to observe the good noise suppression for zero to 20 GHz frequency range. For the reduction of SSN, a new design of 2×8 two-dimensional EBG structure is introduced. The ground plane with dimensions of 26.9 mm $\times$ 55.6 mm is designed on X axis. The middle layer is substrate layer, i.e., FR-4 is created with dimensions of 26.9 mm $\times$ 55.6 mm with 0.8 mm thickness on Y axis. Wave port excitation to the designed ports (Port1 and Port 2) is applied in the simulation. Finally, boundary condition to the ground and EBG plane were applied. The power and ground plane of EBG structure work like a parallel plate waveguide. The change in current consumption causes the excitation of one mode or modes in parallel plate waveguide. Because of this phenomenon, voltage wave propagates away from the excitation point. These waves cause noise suppression on the board.
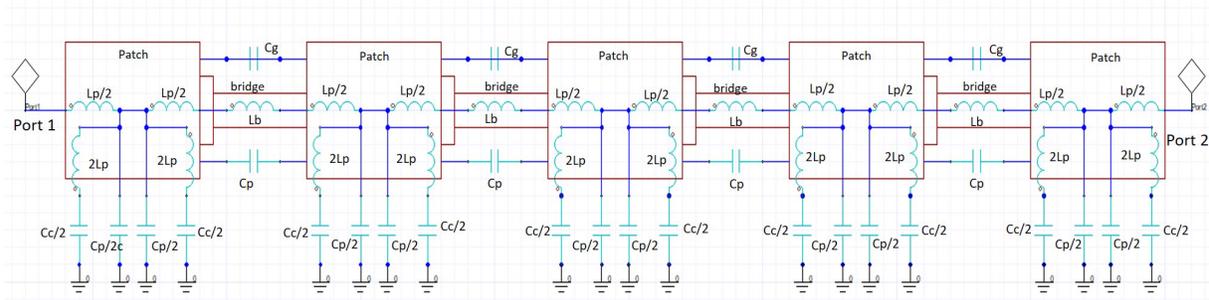
(a) Equivalent circuit model of Proposed structure
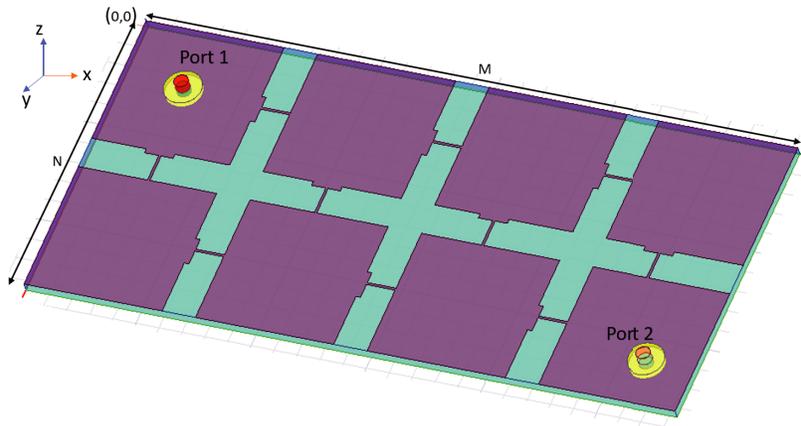
(b) 3D view of proposed structure

Figure 3. (a) Equivalent circuit model of proposed structure from port 1 to port 2, (b) 3D view of proposed structure.

Comparative simulation results are in scattering parameter form of reference plane and proposed EBG design as shown in Figure 4. From simulated results, the proposed structure achieves wideband noise mitigation in comparison with solid reference with 3.13 GHz to 5.47 GHz for bandgap-I and another range from 6.09 GHz to 11.40 GHz for bandgap-II at -30 dB.
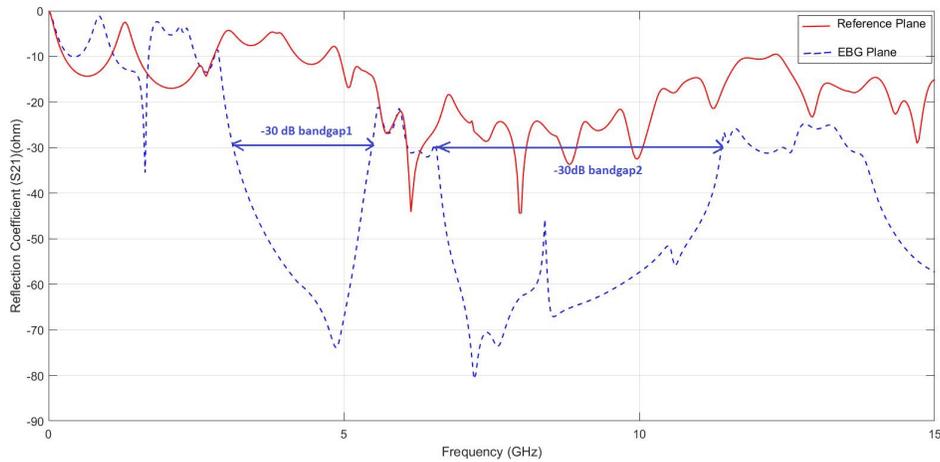

Figure 4. Simulation comparison of frequency spectrum of S_{21} of proposed planar 2D EBG design and reference plane.

4. POWER INTEGRITY (PI) OF THE PROPOSED STRUCTURE

System performance can be checked by S-parameters and input impedance parameter. Self-impedance (Z_{11}) and transfer impedance (S_{21}), parts of Z parameter, are used for low impedance evaluation. Target impedance should be below a specific impedance to maintain power integrity in a system [31, 32]. There are resonance modes due to cavity effects in power plane, which requires to keep the impedance of a system below target impedance. Decoupling capacitors cause self resonance, are not sufficient for suppression of wide bandgap, and provide low impedance as given in [33] and [34]. Decoupling capacitance has lead inductance, so it is difficult to get wide range mitigation for the GHz band.

In higher frequency range, EBG structures are used to control impedance by damping the cavity modes for larger range of frequencies. The self-impedance of reference plane and proposed EBG plane is shown in Figure 5, to compare the effect of damping of cavity modes in the proposed EBG design. We observe that more cavity modes are damped in EBG plane than reference plane. Input impedance is more in reference board due to power bus resonance, while input impedance is less in proposed EBG structure with reduction in power bus resonance.
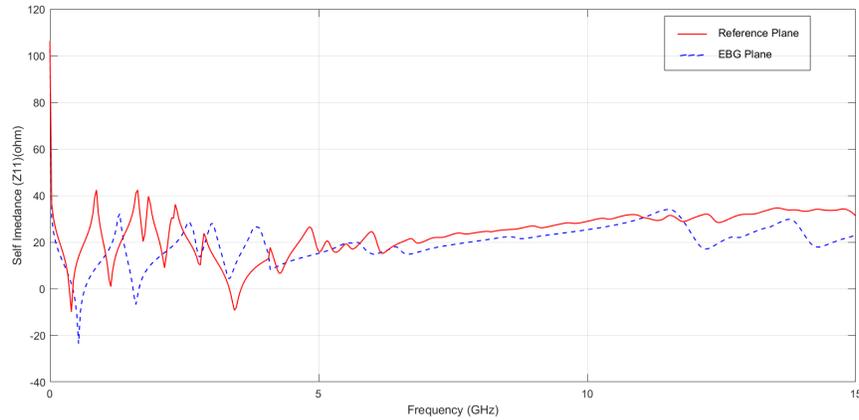

Figure 5. Self-Impedance (Z_{11}) of Proposed 2D EBG and reference plane.

5. SIGNAL INTEGRITY (SI) OF THE PROPOSED STRUCTURE

It is required to check the signal transmission characteristics of the designed structure to get the effect of suppression of SSN [35]. Eye diagram shows the impact of noise on system performance. Eye diagram provides visual representation of signal quality in high-speed designs. In this paper, MATLAB software is used to simulate eye diagrams. Eye diagram is specifically used for analyzing the signal integrity of designed structure and the reference board. Touchstone file is imported from HFSS simulator. Imported data calculation in terms of transfer function and rotational function is done with number of
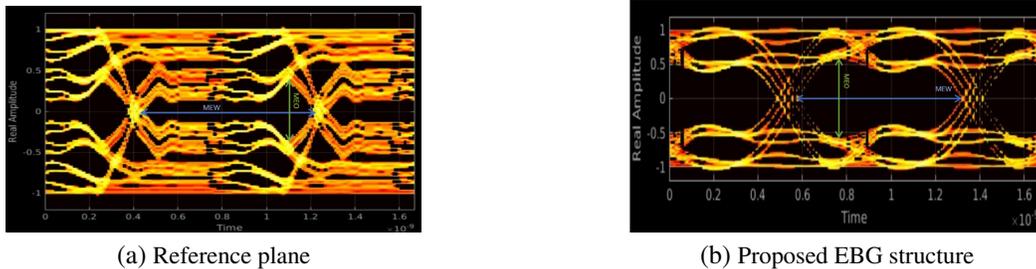

(a) Reference plane

(b) Proposed EBG structure

Figure 6. Simulated eye diagrams for (a) reference plane, (b) proposed EBG structure.

poles. The comparison of frequency response of the rotational object to original data has been done. Finally, we selected and plotted an eye diagram based on the response of a rotational function object to a random 50 Mbps pulse. Eye diagrams for reference board are in Figure 6(a) for reference board and Figure 6(b) for proposed EBG structure. Eye diagram measurements are obtained in terms of amplitude measurements and time measurements. Maximum eye opening (MEO) shows noise voltage and maximum eye width (MEW), gives timing jitter which are important parameters for checking eye pattern quality. "Reference plane in Figure 6(a) and proposed structure in Figure 6(b) show MEO = 0.1 V, MEW = 0.57 ns and MEO = 1.08 V, MEW = 0.63 ns, respectively. Comparison Table 2 gives greatly improved results of the proposed structure for MEO, MEW, and also about good SNR compared to reference board.

Table 2. Comparison of eye diagram measurements.

Eye Measurement	Parameters	Reference Plane	Proposed EBG plane
Amplitude measurement	Eye Height	0.1 V	1.08 V
Amplitude measurement	Vertical Opening	0.1 V	1.08 V
Time measurement	Eye Width	0.57 ns	0.63 ns
Time measurement	Horizontal Opening	−0.84 ns	−0.74 ns

6. HARDWARE IMPLEMENTATION AND VALIDATION OF PROPOSED STRUCTURE RESULTS

The proposed EBG and reference plane have been fabricated as a hardware structure. The two fabricated structures are shown in Figure 7(a) and Figure 7(b), and all the dimensions are mentioned in Table 1. One output receiver port "2" is at (22 mm, 52 mm) and one input port "1" at (5 mm, 5 mm). SMA power connectors are connected with input and output ports. Scattering parameter S_{21} measurement has been checked with the help of Agilent Field Fox Vector Network Analyzer (VNA) 14 GHz to validate the accuracy of Ansoft HFSS simulations.

(a) Reference plane   (b) Proposed EBG structure

Figure 7. Photo of fabricated structures, (a) reference plane, (b) proposed planar EBG structure.

It is observed that the measurement of scattering parameters obtained using the VNA experimental setup is shown in Figure 8. Measured results of reference board and designed EBG structure are in Figure 9. Blue dotted line stands for the proposed structure, and red line represents the reference board. From the hardware results, the bandgap of proposed structure provides SSN suppression from 3.13 GHz to 5.47 GHz for bandgap-I and another range from 6.09 GHz to 11.40 GHz for bandgap-II at −30 dB, in comparison of reference board. Similar ranges are obtained in the simulations results as shown in Figure 4.

The validation of simulated and measured results of designed structure is observed in Figure 10. Figure 10 shows the insertion loss of the simulated proposed EBG plane as a blue dotted line and
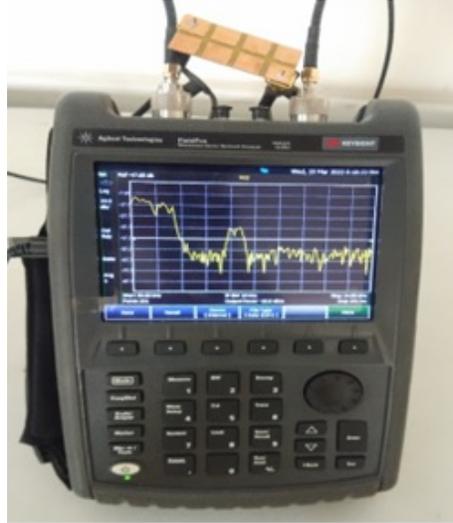
Figure 8. Fabricated structure measurement setup for Frequency spectrum of S_{21} of Proposed planar design.
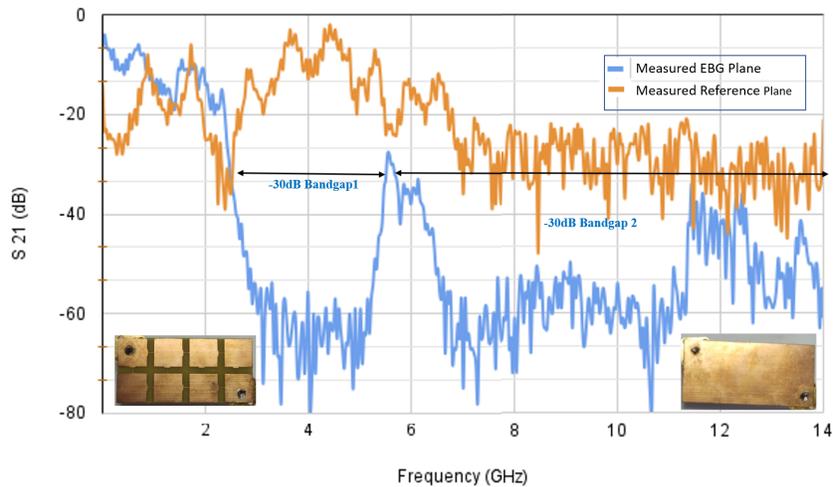

Figure 9. Insertion loss (S_{21}) VNA results comparison between proposed EBG plane and Reference board.

the measured proposed hardware EBG structure as a red line. This gives reflection coefficient (S_{21}) with good agreement between the two results. It is observed that the designed hardware provides almost similar simulated results and measured results, and it shows little difference due to various test environment and processing errors.

Compared to the reference plane, the proposed structure demonstrates the successful suppression of SSN. The frequency range is between 2 GHz and 14 GHz provided by the proposed structure for power and ground continuous plane. This will be useful in high-speed circuit designs.

The proposed structure is compared with published results in Table 3. Ref. [26] used 13.7 mm of unit cell and gave 3.26 GHz bandwidth. Ref. [27] used 12.7 mm of unit cell, with 4.03 GHz. Ref. [33] had 15 mm patch size with 2.97 GHz bandgap. The proposed structure has 12 mm patch size with 8.27 GHz bandwidth, and good bandwidth improvement is observed with the noise suppression within 2 GHz to 20 GHz.

Table 3. Proposed structure comparison with the published results.

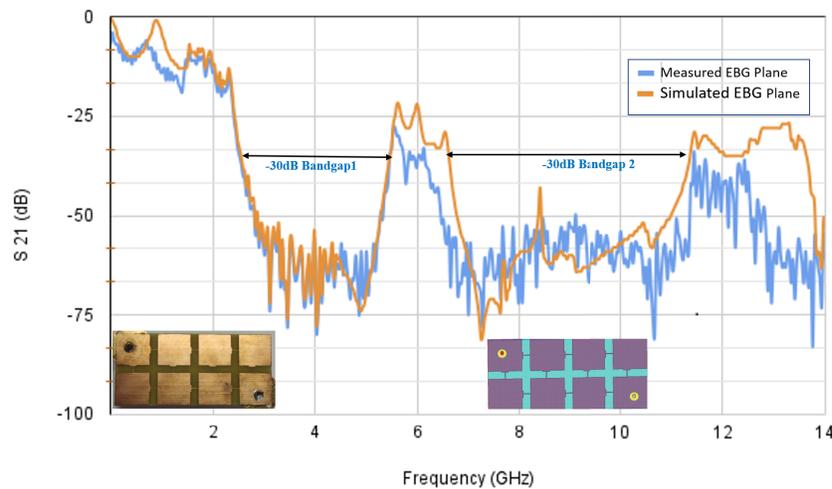| EBG Structure	Patch size	Suppression Depth = −30 dB Lower frequency	Suppression Depth = −30 dB Higher frequency	Bandwidth
Ref. [26]	13.7 mm	2.95 GHz	6.21 GHz	3.26 GHz
Ref. [27]	12.7 mm	2.23 GHz	6.26 GHz	4.03 GHz
Ref. [33]	15 mm	2.21 GHz	5.18 GHz	2.97 GHz
Proposed structure	12 mm	3.13 GHz	11.40 GHz	8.27 GHz

Figure 10. Insertion loss (S_{21}) Comparison between simulated proposed EBG plane and VNA measured proposed EBG Plane.

7. CONCLUSION

In this paper, a two-dimensional T bridge structure is proposed for the improvement of signal and power integrity by the mitigation of simultaneous Switching Noise (SSN). Simulated results give good signal and power integrity. The proposed structure gives suppression bandwidth from 2 GHz to 14 GHz with the proper suppression of SSN.

HFSS was used to design and simulate the proposed EBG structure. The results obtained show that designed bridges provide extra inductance, increasing a system bandwidth. In this work, it was found that the proposed EBG structure successfully reduced simultaneous switching noise at −30 dB for bandgap 1 from 3.13 GHz to 5.47 GHz and bandgap 2 from 6.09 GHz to 11.40 GHz.

The size of the proposed structure is small, and it is highlighted that improved signal and power integrity is achieved with this design. The structure is fabricated by current PCB technology, and good agreement of simulated and measurement results is also observed in time and frequency domains for SSN mitigation by the vector network analyzer (VNA). Low cost, compact size, and easy fabrication are the advantages of proposed design useful for future high-speed systems, specially useful in satellite and Radar communication.

REFERENCES

1. Abhari, R. and G. V. Eleftheriades, "Metallo-dielectric electromagnetic bandgap structures for suppression and isolation of parallel-plate noise in high-speed circuits," *IEEE Trans. Microwave Theory and Techniques*, Vol. 51, No. 6, 1629–1639, Jun. 2003.

2. Sievenpiper, D., L. Zhang, R. F. Jimenez Broas, N. G. Alexopolous, and E. Eli Yablonovitch, "High-impedance electromagnetic surfaces with a forbidden frequency band," *IEEE Trans. Microwave Theory and Techniques*, Vol. 47, 2059–2073, Nov. 1999.

3. Huh, S. L. and M. Swaminathan, "A design technique for embedded electromagnetic band gap structure in load board applications," *IEEE Trans. Electromagnetic Compatibility*, Vol. 54, No. 2, 443–456, Apr. 2012.

4. De Paulis, F., L. Raimondo, and A. Orlandi, "IR-drop analysis and thermal assessment of planar electromagnetic bandgap structures for power integrity applications," *IEEE Trans. Adv. Packaging*, Vol. 33, No. 3, 617–622, Aug. 2010.

5. Zhu, H.-R., J.-F. Mao, and J.-J. Li, "Signal and power integrity analysis for the novel power plane of EBG structure in high-speed mixed signal systems," *IEEE International Wireless Symposium (IWS)*, 1–4, Apr. 2013.

6. Zhu, H.-R., Y.-F. Sun, Z.-X. Huang, and X.-L. Wu, "A compact EBG structure with etching spiral slots for ultra-wideband simultaneous switching noise mitigation in mixed signal systems," *IEEE Transactions on Components, Packaging and Manufacturing Technology*, Vol. 9, No. 8, 1559–1567, Aug. 2019.

7. Han, Y., H. A. Huynh, and S. Y. Kim, "Pinwheel meander-perforated plane structure for mitigating power/ground noise in system-in-package," *IEEE Transactions on Components, Packaging and Manufacturing Technology*, Vol. 8, No. 4, 562–569, Apr. 2018.

8. Wu, T. L., C. C. Wang, Y. H. Lin, T. K. Wang, and G. Chang, "A novel power plane with super-wideband elimination of ground bounce noise on high speed circuits," *IEEE Microwave and Wireless Components Letters*, Vol. 15, No. 3, 174–176, Mar. 2005.

9. Kim, K. H. and J. E. Schutt-Ainé, "Analysis and modeling of hybrid planar-type electromagnetic-bandgap structures and feasibility study on power distribution network applications," *IEEE Trans. Microwave Theory and Techniques*, Vol. 56, No. 1, 178–186, Jan. 2008.

10. Shi, L.-F., Z.-M. Sun, G.-X. Liu, and S. Chen, "Hybrid-embedded EBG structure for ultrawideband suppression of SSN," *IEEE Trans. Electromagnetic Compatibility*, Vol. 60, No. 3, 747–753, Jun. 2018.

11. Shi, L.-F. and H.-F. Jiang, "Vertical cascaded planar EBG structure for SSN suppression," *Progress In Electromagnetics Research*, Vol. 142, 423–435, 2013.

12. Shi, L.-F., K.-J. Li, H.-Q. Hu, and S. Chen, "Novel L-EBG embedded structure for the suppression of SSN," *IEEE Trans. Electromagnetic Compatibility*, Vol. 58, No. 1, 519–520, Feb. 2016.

13. De Paulis, F., A. Orlandi, L. Raimondo, and G. Antonini, "Fundamental mechanisms of coupling between planar electromagnetic bandgap structures and interconnects in high-speed digital circuits. Part I — Microstriplines," *Proc. EMC European Workshop*, 1–4, Athens, Greece, Jun. 11–12, 2009.

14. Keshwani, V. R., P. P. Bhavarthe, and S. S. Rathod, "Eight shape Electromagnetic Band Gap structure for bandwidth improvement of wearable antenna," *Progress In Electromagnetics Research C*, Vol. 116, 37–49, 2021.

15. Chung, D., T. H. Kim, C. Ryu, E. Engin, M. Swaminathan, and J. Kim, "Effect of EBG structures for reducing noise in multi-layer PCBs for digital systems," *Proc. IEEE 15th Conf. Electr. Perform. Electron. Packag.*, 253–256, Oct. 23–25, 2006.

16. Bansode, M. R., R. Dahatonde, and S. S. Rathod, "Simultaneous switching noise reduction in high speed circuits," *IEEE International Conference on Communication information and Computing Technology (ICCICT)*, 1–4, Jun. 25–27, 2021.

17. Kapure, V. R., P. P. Bhavarthe, and S. S. Rathod, "A switchable triple-band notched UWB antenna using compact multi-via electromagnetic band gap structure," *Progress In Electromagnetics Research C*, Vol. 104, 201–214, 2020.

18. Shahparnia, S. and O. M. Ramahi, "Miniaturized electromagnetic bandgap structures for broadband switching noise suppression in PCBs," *Electron. Lett.*, Vol. 41, No. 9, 519–520, Apr. 2005.

19. Bhavarthe, P. P., S. S. Rathod, and K. T. V. Reddy, "A compact dual band gap electromagnetic band gap structure," *IEEE Microwave and Wireless Components Letters*, Vol. 67, 596–600, Oct. 2018.

20. Mohajer-Iravaniand, B. and O. M. Ramahi, "Wideband circuit model for planar EBG structures," *IEEE Trans. Adv. Packag.*, Vol. 33, No. 2, 1345–1354, May 2010.

21. Shinde, S., M. Bansode, P. P. Bhavarthe, and S. S. Rathod, "Suppression of SSN in High-Speed Circuits using 1-D EBG structure," *International Conference on Computing, Communication and Networking Technologies (ICCCNT)*, 1–4, Jul. 2020.

22. Kim, T. H., D. Chung, E. Engin, W. Yun, Y. Toyota, and M. Swaminathan, "A novel synthesis method for designing electromagnetic bandgap (EBG) structures in packaged mixed signal systems," *Proc. 56th Electron. Compon. Technol. Conf.*, 1645–1651, 2006.

23. Wu, T. L., C. C. Wang, Y. H. Lin, T. K. Wang, and G. Chang, "A novel power plane with super-wideband elimination of ground bounce noise on high speed circuits," *IEEE Microwave and Wireless Components Letters*, Vol. 15, No. 3, 174–176, Mar. 2005.

24. Lu, H. M., J. X. Zha, and Z. Y. Yu, "Design and analysis of a novel electromagnetic bandgap structure for suppressing simultaneous switching noise," *Progress In Electromagnetics Research C*, Vol. 30, 81–91, 2012.

25. Ning, C., J. Jin, K. Yang, H. Xie, D. W. Wang, Y. Liao, L. D. Wang, H. S. Chen, E. P. Li, and W.-Y. Yin, "A novel electromagnetic bandgap power plane etched with multiring csrrs for suppressing simultaneous switching noise," *IEEE Trans. Electromagnetic Compatibility*, Vol. 60, No. 3, 733–737, Jun. 2018.

26. Choi, J., V. Govind, and M. Swaminathan, "A novel Electromagnetic Bandgap (EBG) structure for mixed-signal system applications," *IEEE Radio and Wireless Conference*, 243–246, 2004.

27. De Paulis F. and A. Orlandi, "Accurate and efficient analysis of planar electromagnetic band-gap structures for power bus noise mitigation in the GHz band," *Progress In Electromagnetics Research B*, Vol. 37, 59–80, 2012.

28. High Frequency Structure Simlator, www.ansoft.com.

29. Kim, K. H. and J. E. Schutt-Aine, "Analysis and modeling of hybrid planar-type electromagnetic-bandgap structures and feasibility study on power distribution network applications," *IEEE Trans. Microwave Theory and Techniques*, Vol. 56, No. 1, 178–186, Jan. 2008.

30. Swaminathan, M. and A. Ege Engin, *Power Integrity Modeling and Design for Semiconductors and Systems*, Prentice Hall, 2008.

31. Wu, T.-L., H.-H. Chuang, and T.-K. Wang, "Overview of power integrity solutions on package and PCB: Decoupling and EBG isolation," *IEEE Trans. Electromagnetic Compatibility*, Vol. 52, No. 2, 346–356, May 2010.

32. Orlandi, A., B. Archambeault, F. de Paulis, and S. Connor, "Impact of planar EBGs on signal integrity in high-speed digital boards," *IEEE Trans. Electromagnetic Compatibility*, 61–76, 2017.

33. Ning, A. C., J. Jin, K. Yang, H. Xie, D. W. Wang, Y. Liao, L. D. Wang, H. S. Chen, E. P. Li, and W.-Y. Yin, "A novel electromagnetic bandgap power plane etched with multi ring CSRRs for suppressing simultaneous switching noise," *Proc. Asia-Pacific Symp. Electromagn. Compat., Singapore*, 325–328, 2012.

34. Han, Y., Z. Yan, Y. Wang, and T. Rahman, "A novel EBG structure with embedded meander bridge for broadband suppression of SSN," *IEEE Trans. Electromagnetic Compatibility*, Vol. 60, No. 3, 325–328, 2012.

35. Mahmood, F. Z., Y. Toyota, K. Iokibe, K. Kondo, and S. Yoshida, "Power/ground layers with EBG structure and ferrite film for noise suppression and power integrity improvement," *IEEE Electrical Design of Advanced Packaging and Systems Symposium (EDAPS)*, 1–4, 2011.